Review

Ni-Based Catalyst for Carbon Dioxide Methanation: A Review on Performance and Progress

Nur Diyan Mohd Ridzuan [1], Maizatul Shima Shaharun [1,*], Mohd Azrizan Anawar [2] and Israf Ud-Din [3]

1 Fundamental and Applied Sciences Department, Universiti Teknologi PETRONAS,
  Seri Iskandar 32610, Perak, Malaysia; nur_17007454@utp.edu.my
2 Chemical Engineering Department, Universiti Teknologi PETRONAS, Seri Iskandar 32610, Perak, Malaysia;
  mohd_17008379@utp.edu.my
3 Department of Chemistry, College of Science and Humanities, Prince Sattam bin Abdulaziz University,
  Al-Kharj 16278, Saudi Arabia; drisraf@yahoo.com
* Correspondence: maizats@utp.edu.my

Abstract: Catalytic conversion of CO_2 into methane is an attractive method because it can alleviate global warming and provide a solution for the energy depletion crisis. Nickel-based catalysts were commonly employed in such conversions due to their high performance over cost ratio. However, the major challenges are that Ni tends to agglomerate and cause carbon deposition during the high-temperature reaction. In the past decades, extensive works have been carried out to design and synthesize more active nickel-based catalysts to achieve high CO_2 conversion and CH_4 selectivity. This review critically discusses the recent application of Ni-based catalyst for CO_2 methanation, including the progress on the effect of supporting material, promoters, and catalyst composition. The thermodynamics, kinetics, and mechanism of CO_2 methanation are also briefly addressed.

Keywords: CO_2 methanation; nickel-based catalyst; carbon dioxide; hydrogenation

1. Introduction

Today's society faces significant challenges in terms of the energy crisis and climate change caused by global warming. The greenhouse gases (GHGs) which are responsible for the warming of the earth comprise approximately 68% carbon dioxide (CO_2) [1]. Apparently, the natural equilibrium of CO_2 is being disturbed as the concentration of anthropogenic sources increases with over 30 Gt emissions a year [1]. This primarily stemmed from the burning of fossil fuel and coal, as well as the industrial sector [2,3]. In order to mitigate the release of CO_2 into the atmosphere, studies have been focusing on two approaches; to capture and store CO_2 or to recycle the CO_2 into valuable energy-bearing compounds [4,5]. The carbon capture and storage (CCS) is an interesting method that has been utilized by several oil and gas companies to reduce the CO_2 release. Moreover, CO_2 can also be retrieved and utilized as supercritical carbon dioxide for industrial chemical processes [6–8]. CO_2 conversion into valuable products is also assuring, because it can reduce CO_2 emissions and is more profitable for the industries involved with environmental issues [9,10], is also an alternative for hydrogen storage systems and is a renewable energy source via power-to-gas (P2G) technology.

The P2G process chain is the future renewable energy system in which the energy is transformed into storable methane [11]. Figure 1 shows the principle and application of P2G technology. Hydrogen (H_2), is produced by water electrolysis and converted into methane by reacting with CO_2 sourcing from the retrieval of industrial processes [12]. Methane is a component of synthetic natural gas (SNG) which has high volumetric energy content. The application of CH_4 ranges widely from heating in buildings, transportation, and electricity generation in gas turbines to the combination of heat and power plants as well as feedstock for the chemical industry [13,14].
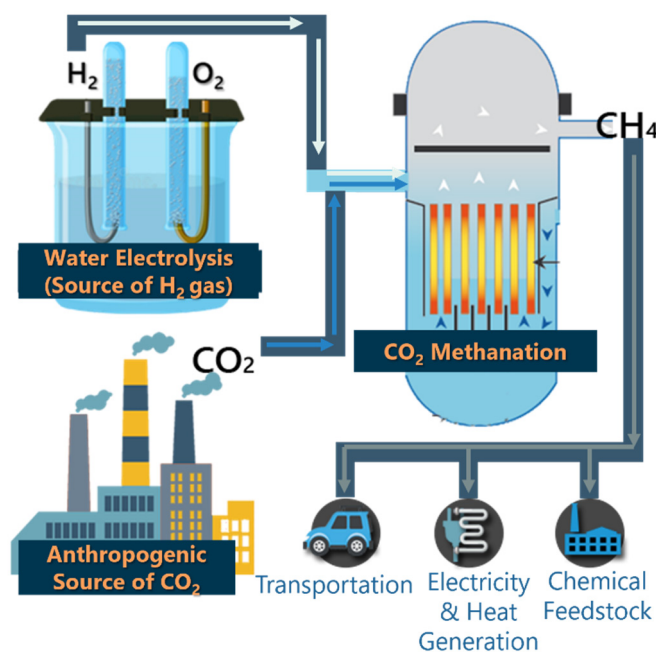
Figure 1. Power-to-gas technology.

Extensive research works attempted to improve CO_2 methanation via the Sabatier reaction, with the works being focused on the development of active catalysts. The aim of catalyst development is to improve the percentage of CO_2 conversion and CH_4 selectivity [2,15]. Metals that have been previously used for CO_2 methanation are various with nickel (Ni) being the most widely studied under various experimental conditions due to its relatively high performance to cost ratio [16]. The catalytic activity of Ni can be enhanced by supporting it onto high surface area material and introducing a second metal, which will promote CO_2 conversion. The selection of the supporting material is crucial because it has a significant influence on the physicochemical properties of the Ni active phase, and it can affect CO_2 adsorption [17]. Thermostable, high surface area and porous materials are effective to avoid the coalescence of Ni particles. Furthermore, various metals have been used together with Ni as a bimetallic catalyst to enhance the efficiency of CO_2 methanation by improving the coke-resistance property of the catalysts. As demonstrated in previous research for bimetallic catalysts, a small amount of the second metal will interact with Ni, thereby changing the dispersibility and reducibility of the catalysts [18]. Hence, a reaction can be efficiently carried out at a lower temperature with improved CH_4 selectivity.

Overall, previous research had shown that the supporting material, promoter's element, and catalyst composition resulted in different characteristics of Ni-based catalysts which correlated to its activity in CO_2 methanation [19,20]. Herein, this present review summarizes recent advancements in the research and development of Ni-based methanation catalysts where reaction thermodynamics and the mechanistic pathway of CO_2 methanation, and the effect of supporting materials and promoters are outlined. Further, the types of methanation reactors and the mechanism are also discussed.

2. Thermodynamics and Kinetic Aspect of CO_2 Methanation

The key reaction for methane production was discovered in 1902 by Paul Sabatier and Jean-Baptiste Senderens [12], which is described in Equation (1) (Sabatier reaction). It was widely accepted that CO_2 is first converted into CO intermediate via a reverse-water gas shift reaction (R2) [17,21] before CH_4 is produced from CO methanation (R5) [17,21]. Another side reaction producing coke may also occur in R3, R6, and R7, which will affect the purity of the products. These possible side reactions involved in CO_2 methanation, as in Table 1, were determined according to available literature [13,22,23], and their standard enthalpy, $\Delta H°$, and standard Gibbs free energy, $\Delta G°$, were obtained from the FACTSAGE 7.3 software. Six

possible side reactions that may occur are listed in Table 1, with R1, R2, and R4 regarded as independent reactions.

Table 1. List of CO_2 methanation and possible side reactions.

Equation	Reaction Label	ΔH_{298K} (kJ/mol)	ΔG_{298K} (kJ/mol)
(1)	R1	−165.01	−113,618
(2)	R2	41.16	28,674
(3)	R3	−90.14	−90,143.1
(4)	R4	172.47	120,153.5
(5)	R5	−206.17	−142,292
(6)	R6	−131.3	−91.48
(7)	R7	77.91	42.28

Hence, upon the completion of the methanation reaction, there will be a mixture of products, side products, and reactant-in-equilibrium (CO_2, H_2, CO, CH_4, H_2O, and C). In order to predict the optimal reaction condition to achieve high CO_2 conversion and CH_4 selectivity, thermodynamic analysis is therefore useful. This is because experimental results revealed that CO_2 methanation is sensitive to many operational factors, such as temperature, pressure, and the composition of reactants. Theoretically, the overall reaction in Equation (1) is favored at a lower temperature, elevated pressure and H_2/CO_2 ratio equal to or more than the stoichiometric ratio [22].

$$CO_2 + 4\,H_2 \rightarrow CH_4 + 2\,H_2O \tag{1}$$

$$CO_2 + H_2 \rightarrow CO + H_2O \tag{2}$$

$$CO_2 + 2\,H_2 \rightarrow C + 2\,H_2O \tag{3}$$

$$CO_2 + C \rightarrow 2\,CO \tag{4}$$

$$CO + 3\,H_2 \rightarrow CH_4 + H_2O \tag{5}$$

$$CO + H_2 \rightarrow C + H_2O \tag{6}$$

$$CH_4 \rightarrow 2\,H_2 + C \tag{7}$$

2.1. Effect of Reaction Temperature

To understand the effect of temperature towards the reaction system, equilibrium constant (K) of the CO_2 methanation and other side reactions under the isothermal standard state in the temperature range of 423 K to 723 K from Equation (8), the values were obtained using FACTSAGE 7.3 software.

$$\Delta G = -RT \ln K \tag{8}$$

The plot of Ln K_{eq} versus temperature (Figure 2) shows that the methanation reaction (R1) is suppressed with the increase in temperature due to the exothermic nature of the reaction. All exothermic reactions (R3, R5, and R6) that may accompany CO_2 methanation also show suppression with a temperature increase, meanwhile, the endothermic reaction (R2, R3, and R4) increases. The CO_2 methanation reaction possessed a $\ln K_{eq}$ value of 0 at 860 K, suggesting that only a temperature lower than 860 K will shift the reaction to produce more products. Due to the high $\ln K_{eq}$ value, high conversion of CO_2 can be achieved in the lower temperature range and at high pressure. Apart from that, the side reaction may also reduce methane production [22]. This trend has been proven correct in many experimental data as well. A work by Zhang et al. [24] shows a lower catalytic activity for CO_2 methanation at high temperatures, meanwhile, R2 (RWGS reaction) increases as these two reactions are competitive reactions.
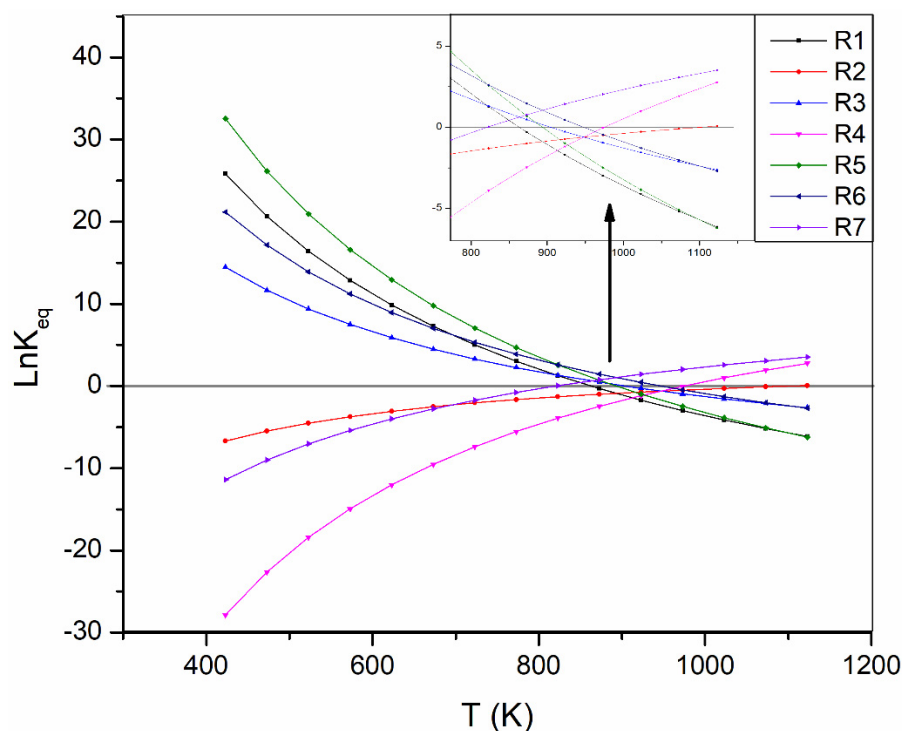
**Figure 2.** LnK_{eq} versus T plot for R1–R8. (P = 1 atm, H_2/CO_2 ratio = 4).

Previous studies showed that CO_2 methanation using Ni-based catalysts were commonly carried out in the temperature range of 523 K to 723 K [25–27]. Recently, several studies attempted low-temperature methanation with the temperature beginning from 423 K by using selective catalysts [28–30] and/or a three-phase reactor. This is to ensure the temperature used will not suppress the CH_4 yield due to the domination of CO byproducts from R2 as its K_{eq} increases at elevated temperatures. Additionally, reactions carried out at a temperature higher than this range can cause sintering of catalyst and increase in carbon deposition, resulting in catalyst deactivation.

However, considering the kinetic limitation of the catalyst and the challenges for the reaction to achieve equilibrium at a lower temperature, CO_2 methanation might be less efficient at a temperature lower than 423 K. In terms of the kinetic aspect, temperature increase promotes a higher rate of reaction. In their study, Lefebvre et al. reported the pronounced influence of temperature on the CO_2 reaction rate in a two-phase fluid-bed reactor. The activation energy of CO_2 methanation is 73–78 kJ/mol under the presence of Ni catalyst. As the temperatures are varied ranging from 200 to 300 °C, the CO_2 reaction rate is almost double for each temperature increase of 20 K. Moreover, [31], with regards to previous studies on CO_2 methanation, the optimal operating window is at a temperature of around 200 °C to 500 °C, as shown in Table 2. The maximum temperature of 500 °C is the maximum used to avoid the reverse reaction and at the same time, to compensate for thermodynamic and kinetic limitations. Moreover, temperature control in the reactor is of great importance, too, since an exothermic methanation reaction may cause the apparent temperature to increase in large-scale operations [32].

2.2. Effect of Reaction Pressure

In order to understand the effect of pressure on the extensive properties of CO_2 methanation, the calculation for ΔG and K_{eq} at different pressures was conducted. Figure 3 presents the value of LnK_{eq} at different P for CO_2 methanation. It is evident that the LnK_{eq} values show a logarithmic increase with increasing pressure, accompanied by an increase in reaction spontaneity. This phenomenon can be explained by the Le' Chatelier principle. [33]. CO_2 methanation is a volume-reducing reaction from 5 to 3 molecules; hence, increasing

the pressure will result in lower volume, favoring the product over the reactant. As the increase is logarithmic, the effect of pressure on CO_2 methanation became less significant at higher pressure. Thus, the pressure range of 1 atm to 30 atm is commonly used for CO_2 methanation reactions. Elevating the pressure in the reactor increases the lnK_{eq}; its K_{eq} value reflects higher CH_4 yield and CO_2 conversion effectively up to 30 atm. From the kinetic point of view, inlet H_2 partial pressure will influence the reaction rate as well, as shown in a previous study [31]. At 300 °C, the reaction rate can be enhanced up to 70% when $P_{H_2,in}$ is increased from 1 bar to 4 bar in a fixed-bed reactor. Meanwhile, at the same temperature, the inlet CO_2 partial pressure $P_{CO_2,in}$ has a significantly lower influence on the CO_2 reaction rate with only a 17% increase when $P_{CO_2,in}$ rises from 0.75 bar to 1.25 bar.
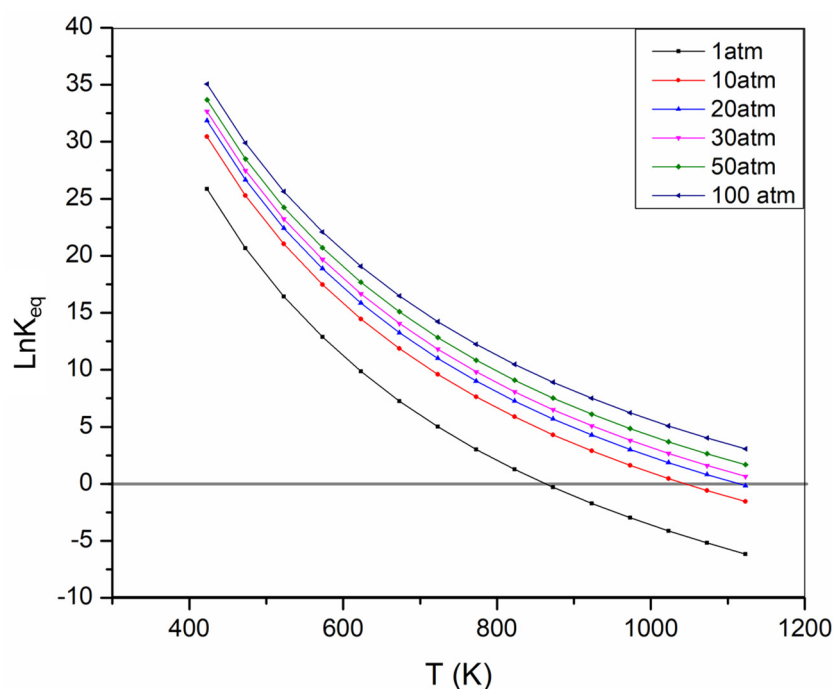
Figure 3. LnK_{eq} versus T plot for CO_2 methanation (R1) at different pressure (H_2/CO_2 ratio = 4).

Even though the thermodynamic and kinetic aspect of reaction indicates a higher conversion and rate at higher pressure, it shall be noted that extreme reaction conditions are also less opted in the industry due to instrument limitation and high energy consumption [11,14]. Hence, considering the thermodynamic aspect and instrument limitation, the operating window commonly used is 1 atm to 30 atm in which a two-phase reactor commonly employs atmospheric pressure, meanwhile, the three-phase reactor employs a higher pressure to improve gas solubility [34]. According to Gao et al. [35], the use of a pressure slurry reactor is a potential aspect to improve the methanation process because this type of reactor can operate at high pressure [36], which will improve CO_2 conversion.

2.3. Effect of Reactant Composition

Some thermodynamic analyses had also been carried out to understand the effect of the reactant composition (H_2/CO_2) ratio on CO_2 methanation. The fraction of the end product component varies differently with different H_2/CO_2 ratios [13]. When the ratio is increased from 1 to 4 at the same temperature and pressure, CH_4 yield increases because the condition is selective towards reaction (1). A further increase to a ratio of 6 does not result in effective improvement both for CO_2 conversion and CH_4 selectivity. Hence, most of the methanation research uses a H_2/CO_2 ratio of 4. CO byproducts decrease at higher temperatures when the 4:1 ratio of H_2/CO_2 is used. Moreover, coke formation was suppressed to a great extent as R3 is disfavored at a high stoichiometric ratio. Gao et al. [22] suggested that this is due to water formation in CO_2 methanation, which suppresses carbon deposition.

Conclusively, it can be said that high pressure, low temperature, and a proper H_2/CO_2 ratio will result in high CO_2 conversion and CH_4 selectivity. The optimization study is important to ensure the condition is far from the optimal range of the formation of CO and C. Complexity of the Sabatier reaction also relates to the high kinetic barrier of the eight-electron process [37]. Therefore, the development of an active and stable catalyst to achieve acceptable rates and selectivity is still a challenge [38].

3. Ni-Based Catalyst

Over the past decades, considerable work has been done with the aim to develop thermally stable methanation catalysts with high activities at low temperatures and this has been demonstrated by a burgeoning number of publications [2]. Heterogeneous catalysts based on transition metals from group VIII were commonly employed. Methanation reaction involves CO_2 adsorption and dissociation before reacting with H_2 [39] in which the reaction rate is closely related to a reactant dissociation on the catalyst. In a study by Bligaard et al. [40], a volcanic relationship was observed between the activities of methanation versus dissociative CO adsorption energy with Ru possessing the highest activity. Similar findings on high Ru activities for methanation have been observed in other studies [41,42]. A comparative study was carried out by Garbarino et al. [41] on the performance of 3 wt% Ru/Al_2O_3 and 20 wt% Ni/Al_2O_3 commercial catalysts for CO_2 methanation. The data, as reported, confirmed that the catalytic performance of the Ru-based catalyst was prominent in that a 96% CH_4 yield could be achieved without CO co-production at a 300 °C operating temperature. This outperformed the performance of the Ni catalyst in which a maximum CH_4 yield of 80% can be achieved with some CO co-production at 400 °C.

Even though Ru is evidenced to be an active and stable metal for methanation, Ni has attracted more attention, as its price is comparatively 100 times cheaper than Ru with fairly good activity [43]. Ni is one of the most investigated metals for CO_2 methanation due to its reasonable combination of good characteristics and price; hence, making it suitable for commercial use. However, the primary challenges of using Ni in industrial catalytic processes include carbon deposition, sintering of the particle formation of $Ni(CO)_4$ and severe sulfur poisoning during SNG production, which is carried out at elevated temperatures [37]. Consequently, this relates to the low stability of the catalyst, causing it to have a short lifetime and low reusability. Deposition and metal sintering will result in catalyst deactivation [44]. Therefore, in order to reach high CO_2 conversion and CH_4 selectivity at low temperature using Ni, selection of catalyst support [45–48], the addition of a second metal or promoter [18,44,49], and the modification of the synthesis method and parameters [4,50] have been intensively studied. This is because different compositions and methods to produce the catalyst will result in different characteristics of the material which are highly correlated with the performance of the catalysts. Supporting Ni onto support will help to improve the dispersion, and the anchoring will reduce Ni particle sintering. Then, the addition of a second metal-producing bimetallic catalyst can improve CO_2 methanation through a synergistic effect and the ability to resist carbon deposition. Modification of the synthesis method was studied to produce catalysts with high surface area and low particle size [51]. Table 2 summarized the performance of Ni-based catalysts in the past years.

Table 2. Summary of Ni-based catalyst and its performance for CO_2 methanation.

Reference	Second Metal	Support	Synthesis Method	Optimum Temperature (°C)	CO_2 Conversion (%)
[52]	-	Al_2O_3	Wetness Impregnation	450	~65.0
[53]	Fe	Al_2O_3	Co-Precipitation	220	58.50
		ZSM-5			76.0
		SBA-15			73.0
[46]	-	MCM41	Impregnation	400	65.0
		Al_2O_3			70.0
		SiO_2			66.0
[47]		SiO_2/rGO	Vapor Deposition	470	83.7
[54]	Zr	Al_2O_3	Co-Precipitation	400	77.0
[55]	-	SiO_2/Al_2O_3	Sol-gel	350	82.38
[56]	La	Zeolite	Wetness Impregnation	450	73.0
[57]	-	SiO_2	Impregnation	400	80.0
[58]	-	ZrO_2	Wetness Impregnation	450	60.0
[27]	-	Al_2O_3	Hydrolysis	350	77.0
[59]	K	ZrO_2	Wetness Impregnation	450	60.0
	La				35.0
[60]	Ce	MCM-41	Precipitation	380	85.6
[61]	Na	CeO_2	Impregnation	290	95.0
	-				60.0
	La				73.0
[25]	Ce	Al_2O_3	Evaporation-induced assembly	400	64.0
	Sm				67.0
	Pr				77.0
[45]	-	Al_2O_3	Impregnation	350	75.0
		Y_2O_3		350	77.0
		ZrO_2		350	76.0
		CeO_2		300	71.0
		La_2O_3		400	53.0
		Sm_2O_3		300	66.0
[62]	-	CeO_2	Impregnation	250	91.0
[63]	-	Al_2O_3	3D-fibre deposition	400	91.0
			Wetness Impregnation	400	74.0
[64]	Cu	SiO_2	Wetness Impregnation	350	55.0
[65]	-	CeO_2	Hydrothermal	300	~90.0
[66]	-	CeO_2	Sol-gel	250	80.5
[67]	-	rGO	Wetness Impregnation	240	51.0
[68]	-	CeO_2	Impregnation	300–350	90.0
[69]	Cu	Hydrotalcite	Co-precipitation	350	86.0
[52]	V_2O_5	MCM-41	Hydrothermal	400	69.3
[70]	Co	Hydrotalcite	Co-precipitation	300	77.0
[71]	-	Zeolite	Wetness Impregnation	400	85.0
[72]	Cr	Al_2O_3	Solid-state	350	80.5
[73]	Y_2O_3/Mg	MCM-41	Co-precipitation	400	65.5
[74]	-	Al_2O_3	Evaporation-induced sel-assembly	350	83.0
[75]	-	Al_2O_3	Hydrothermal	325	~70.0
[76]	Ce	rGO	Impregnation	350	84.5
[77]	-	Phyllosilicate	Hydrothermal	330	~80%

4. Effect of Support

Even though Raney® Ni or Ni nanoparticles are active for carbon dioxide methanation, most of the studies involve the use of Ni nanoparticles supported on high surface area materials [35]. The strategy of adding support to the catalyst system can be explained by the fact that the support has a significant influence on the catalyst properties in a few aspects. Firstly, the presence of support can improve the dispersion of Ni nanoparticles; hence, the active sites will increase. In addition to that, since the adsorption of CO_2 onto the catalyst

is considered to be the critical step, the addition of support onto the Ni-based catalyst can improve adsorption [4]. Then, it can also decrease the sintering of nanoparticles by establishing a physical anchor between the support and Ni particles [78]. The activity and selectivity of supported Ni are strongly influenced by the amount of Ni metal loading, size of dispersed Ni metal particles, metal-support interaction, and the composition of support. Referring to Figure 4, often, ceramics supports, such as silica [50], mesostructured silica nanoparticles (MSN), aluminium oxide [37], and hydrotalcite [79,80] were investigated for CO_2 methanation. Apart from that metal oxide supports, such as ZrO_2, TiO_2, and CeO_2 are also widely studied. In more recent studies, the use of carbon-based support has begun to gain considerable attention in the CO_2 methanation field [76,81].
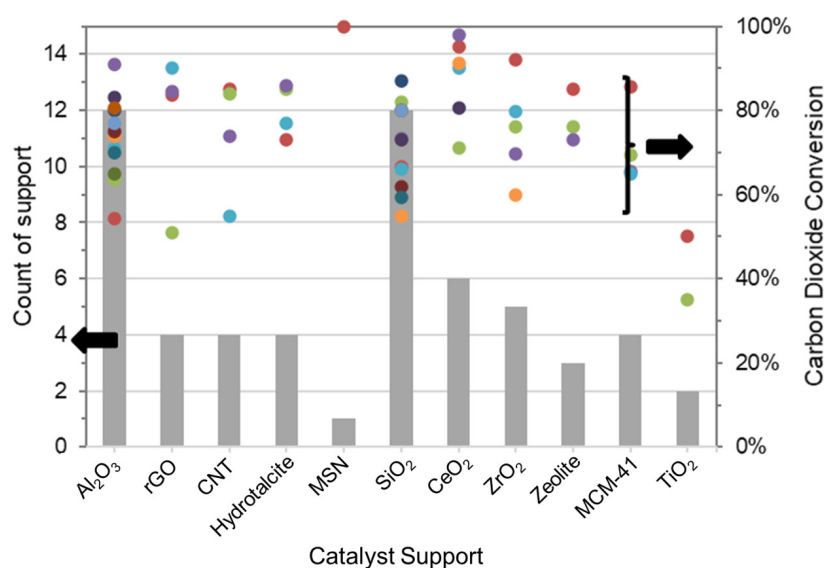
Figure 4. Literature survey plot for catalyst support and their CO_2 conversion.

4.1. Ceramic Support

Alumina (Al_2O_3) was commonly reported as support due to its ability to improve CH_4 selectivity, low cost, and ease of availability [12]. A comparative study using unsupported Ni nanoparticles and Al_2O_3-supported Ni catalyst for CO_2 methanation, by Riani et al. [82], found a notable improvement in catalytic performance when Ni is supported on Al_2O_3 with a 125 wt% loading. In terms of CO_2 conversion, Ni/Al_2O_3 possessed a 71% conversion at 500 °C, whereas Ni nanoparticles have a 6% conversion under the same condition. The poor activity of Ni nanoparticles was caused by a lack of formation of carbon-stabilized hexagonal nickel in the experiment. Spent Ni/Al_2O_3 catalyst shows that there is lesser agglomeration, proving the importance of support to prevent sintering. CO_2 methanation was postulated, by this group, to occur on the alumina support at the basic site in a larger fraction whilst Ni was responsible for H_2 activation. However, this postulation contradicts the hypotheses of several other studies [24,25]. Zhang et al. [24] studied the impacts of Ni loading on reaction intermediates formed in CO_2 methanation. It was found that the variation of Ni loading affects the mechanism and intermediates formed. This suggested the CO_2 conversion occurred on the Ni surface and Al_2O_3 only functions to create the metal-support interaction so metal agglomeration can be reduced. Another study indicated that the activation of CO_2 at low temperatures occurred on the second metal. This is because the second metal enhances surface basicity instead of the alumina support [25].

Other studies using Ni/Al_2O_3 catalyst systems without promoters, synthesized from conventional methods, commonly result in CO_2 conversion of 50% to 80% with selectivity above 90% at an optimum temperature of 350 to 450 °C [28,55,63,74,83–86]. The formation of nickel aluminate, $NiAl_2O_4$, and spinel is often observed from the X-ray diffractogram of the catalyst. Zhan et al. [57] and Daroughegi et al. [87] reported that the presence of $NiAl_2O_4$ results in high reduction temperature (lower reducibility) of the Ni active phase due to

strong metal-support interaction; hence, CO_2 methanation activity decreases. Comparative studies of CO_2 methanation between Al_2O_3 support and other supports have been reported as well, in the past years. Under low-temperature conditions (220 °C), the performance of catalyst with Al_2O_3 support is low. It was reported that only 58.5% CO_2 was converted into methane compared to a 76% and 73% conversion by ZSM-5 and SBA015 supported catalysts, respectively [53]. Even though Al_2O_3 is highly abundant and cost-effective, past studies conclude that the Al_2O_3 works best only at high temperatures, and it creates a strong metal-support interaction that requires high reduction temperatures of which are less favorable in industry.

Under the presence of Al_2O_3 support, higher CO_2 conversion can be achieved from the tailoring of the synthesis method and the addition of promoters. A study by Danaci et al. [63] shows significant improvement in Ni/Al_2O_3 performance with up to 91% CO_2 conversion using Ni/Al_2O_3 fabricated from the three-dimensional fiber deposition (3DFD) technique. As this method is new, mass production might be one of its limitations due to its high cost.

Even though Ni/Al_2O_3 shows higher catalytic activity than unsupported Ni nanoparticles, it suffers from severe carbon deposition and poor stability, as high temperatures are commonly used [17]. Another major limitation displayed by Al_2O_3 is the occurrence of structural changes due to the presence of high-temperature steam produced from the methanation reaction (Equation (1)) [88]. When there is H_2O at high temperature, γ-Al_2O_3 was found to be converted to hydrated boehmite (AlOOH) which decreases the surface area and acidity leading to deactivation. Apart from that, Ni particles usually experienced sintering and agglomeration. As explained by Bai et al. [89], the deactivation mechanism of the Ni/Al_2O_3 catalyst began with the coalescence of Al_2O_3-encapsulated Ni particles, which resulted in a decrease in the metal surface area, as evidenced by the result of BET surface area. To overcome these disadvantages, many researchers add promoters consisting of different elements to improve CO_2 methanation using Ni/Al_2O_3 catalysts. This is further discussed in Section 6.

Another widely used ceramic support is silica (SiO_2) due to its high surface area with tailored pore diameters. As a result, metal-support interactions are established between nickel and silica; hence, disfavor the formation of nickel carbide. This consequently results in a better ability of the catalyst to resist coke formation and Ni sintering [78]. As indicated by previous studies of CO_2 methanation using SiO_2 supported catalyst, CO_2 conversion is only around 60% to 75% [38,47,49,50,57]. A higher conversion of 82.38% with above 90% CH_4 selectivity at 350 °C was achieved by Moghaddam et al. [55] where Al_2O_3–SiO_2 composite was used as support for Ni catalyst. The incorporation of SiO_2 as support in Al_2O_3 outperformed the conventional Ni/Al_2O_3 catalyst in which the best performing catalyst is Ni with Al_2O_3/SiO_2 support of a 1:0.5 ratio. This is because Al_2O_3/SiO_2 results in an improvement in catalyst reducibility. The H_2TPR result depicted that there is increasing H_2 consumption with a lower reduction T in the presence of SiO_2. The SiO_2–Al_2O_3 interaction weakened the interaction of Ni species with Al_2O_3 by forming the Ni–SiO_2 interaction to separate NiO from $NiAl_2O_4$ spinel. A similar conversion of approximately 82% was also found by Li et al. [16], using Ni/SiO_2 with modification of the synthesis method and addition of Mg promoter.

Mesostructured silica nanoparticles (MSN) and MCM-41 have recently found a wide interest in heterogeneous catalysis due to their ordered structure with nanosized dimensions. Aziz et al. [2] compared the activity of Ni/MSN to four other supports (MCM-41, protonated Y zeolite, SiO_2, and Al_2O_3) towards CO_2 methanation. Ni/MSN depicted the highest activity (a 64.1% conversion) and CH_4 selectivity (99.9%) with good stability amongst supported Ni catalysts. This result was reported to be due to the high surface area of mesoporous MSN, which provides better Ni dispersion, and a high concentration of basic sites on the MSN, which inhibit coke formation. MCM-41 was found to be the second-highest in ranking for the conversion with X_{CO_2} = 56.5%. However, in a study by Wang et al. [60], Ni-MCM41 has prominently higher activity (X_{CO_2} = 78%, S_{CH_4} = ~95%) at 360 °C. The large difference is probably caused by the different synthesis methods

and reaction conditions used. Overall, SiO_2 demonstrated high CH_4 selectivity but low CO_2 conversion.

Aside from the above, zeolite is also another ceramic support that has gained attention among researchers as a support for the Ni-based methanation catalyst [56,71,90]. Gac et al. [71] reported a lower temperature CO_2 methanation using the Ni/zeolite catalyst system in which CO_2 conversion and CH_4 selectivity show significant improvement. Their study also revolved around in situ DRIFTS to monitor the state of catalysts throughout the reaction. Unfortunately, it was found that the specific surface area decreases and nickel particle size increases with the time-on-stream. Based on their study, the dissociation and adsorption of CO_2 and H_2 occur on the surface of metal. Apart from the materials mentioned in this section, there are also top-notch ceramic materials, such as MSN, MCM-41 and SBA-15 which demonstrated improved activity [46]; however, they are relatively expensive, and the synthesis method of such supports are commonly tedious with high cost. Another major limitation of using ceramic support is that they are irreducible metal oxide; thus resulting in low H_2 consumption [91].

4.2. Metal-Oxide Support

Besides ceramic supports, metal oxides also offer some advantages, such as basic characteristics, high CO_2 adsorption capacity, and high surface area [45]. Among them, zirconia and ceria supports are mostly used as catalyst support for a wide application of catalysis owing to their high thermal stability and high porosity. By supporting 30% Ni on ZrO_2, about 90% CO_2 was converted at 250 °C with ~95% selectivity towards CH_4, as reported by Ren et al. [18]. ZrO_2 was found to have oxygen vacancies, which promote CO_2 dissociation in the catalyst system. Ni/ZrO_2 outperformed the other ceramic support as it can be conducted at a lower temperature of 250 °C with a 90% conversion compared to Ni/Al_2O_3, which reports a lower CO_2 conversion around 50% to 80% at higher temperatures. The high oxygen vacancies which function to improve the ability to disperse Ni are also observed in other metal oxides, such as CeO_2 and Y_2O_3, as reported before [45,62]. The advantage of using metal oxide is that this support can intervene in the reaction by dissociating CO_2 on its surface as well as providing the chemical interaction with Ni catalyst. However, it was agreed that the gap in using metal oxide, such as ZrO_2, is due to its crystal lattice-dependent activities. Different polymorphic structures (monoclinic, tetragonal and cubic) will result in different activities of CO_2 methanation. Based on previous reports, tetragonal ZrO_2 is the functional structure as catalyst support [92,93]. This structure-sensitive performance of ZrO_2 support for CO_2 methanation causes difficulty in the synthesis method to grow a pure or higher composition of tetragonal ZrO_2.

After ZrO_2, ceria (CeO_2) is also widely studied, as shown in the previous literature. Zhou et al. [62] employed CeO_2 as catalyst support, produced via a hard-template method with the aim to understand the role of surface Ni and Ce species in the reaction. In situ characterization is useful to study the mechanism and intermediates for the reaction. The reduction of CO_2 into CH_4 occurred on the Ni surface, in which hydrogen is dissociated. Furthermore, the ceria contains surface oxygen vacancies in which CO intermediates are produced. A study on the comparison of metal-oxide support has been conducted by Muroyama et al. [45], revealing that under similar reaction conditions, the order of methane yield for different supports follows the order of $Y_2O_3 > Sm_2O_3 > ZrO_2 > CeO_2 > Al_2O_3 > La_2O_3$. The catalytic activities of a nickel-based catalyst supported on different metal-oxides can be explained by its basic properties. The trend of catalyst performance is directly correlated to its basicity, as the metal-oxide support serves as a platform for adsorption and dissociation of carbon dioxide. Hence, the more basic the catalyst, the higher the adsorption of acidic CO_2. This study also explains the route for methanation reaction on metal oxide, which took place via the formation of carbon monoxide as the intermediate. Metal-oxide support has also been proven to show better stability compared to Al_2O_3 and SiO_2 [45]. Apart from that, TiO_2 nanoparticles have also been explored as the support for nickel [50,94–96]. As a whole, the general finding on

the use of metal-oxide support is that the mechanism proceeds with the RWGS reaction to produce CO intermediates before CH_4 is produced. CO_2 and H_2 are adsorbed on the support and Ni, respectively.

4.3. Carbon-Based Support

Carbonaceous materials were also investigated as Ni supports in CO_2 conversion studies. Carbon-based supports (CNT and rGO) depicted a high conversion of > 80%, as depicted in Figure 5. In a comparative study by Wang et al. [97], Ni–Ce/CNT depicted better CO_2 conversion (83.8%) and very high CH_4 selectivity (99.8%) than Ni–Ce/Al$_2$O$_3$. Better performance of Ni-based catalyst on CNT support relates to electron donation and facilitation from Ce and CNT; hence accelerating CO_2 activation on the catalyst surface. Due to high thermal stability, CNT-supported catalyst shows better performance in the stability tests.
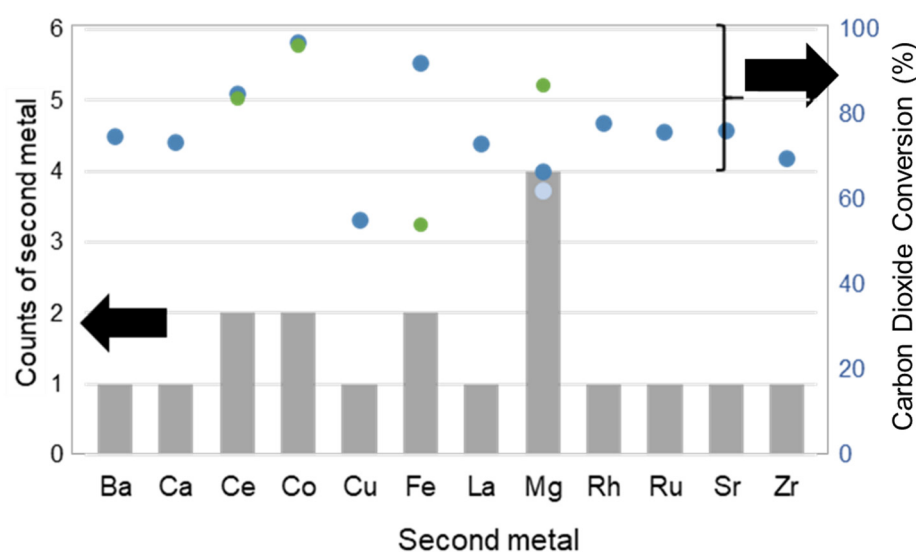
Figure 5. Literature survey plot for second metal and their CO_2 Conversion.

In recent years, graphene has sparked significant attention, both for fundamental aspects and application studies [98] after the breakthrough of the first isolation of single-layer graphene was made in 2004 by Novoselov and Geim [99]. Graphene is an sp^2 hybridized carbon-based material with a hexagonal monolayer network forming a two-dimensional structure [100]. In two-phase reactors, studies showed that the Ni/rGO system can achieve around 80–90% CO_2 conversion [76,81,96]. On the other hand, a CO_2 conversion of 51% was achieved at a low temperature of 240 °C [67]. The presence of free electrons and pi electrons makes graphene a great support, as it can facilitate metal-support interaction, based on the Lewis acid-base interaction. In a study by Mohd Ridzuan et al. [71], the performance of nickel catalyst increases significantly when it is supported by rGO compared to Raney Ni. This is because once supported, the agglomeration was suppressed significantly and new interactions based on the Lewis acid-base interaction of electron transfer between Ni and the support were created. As a result, a higher number of basic sites are produced. The use of carbon-based supports (carbon nanofibers, carbon nanotubes, graphene, etc.) was also widely discussed in other processes of CO_2 conversions, such as the Fischer–Tropsch process [101–103], and CO methanation [104].

Even though there are still limited studies reported on the use of carbon materials as catalyst support for CO_2 methanation, they are projected as a potential material due to their economical reason, high surface area with ample porosity, high thermal, and mechanical stability, and significant selectivity [105]. Hence, further investigations on CO_2 methanation using Ni supported by carbon-based materials are needed.

5. Effect of Second Metal

Further modification of catalyst by adding promoters or second metal into the catalyst system is expected to enhance the CO_2 conversion and CH_4 selectivity, as proven by other studies [49,97,106] because it will intervene in the reaction. The addition of a second metal is important to improve the stability and avoid sintering, hindering the formation of carbon deposits and severe deactivation [13,107]. Therefore, the bimetallic catalyst system has attracted a great deal of attention to enhance the stability and catalytic activity of the nickel-based catalyst [2]. Beforehand, as shown in Figure 5, various second metals namely Fe [44], Zr [4], Pd [38], La [82] and Mg [16,107] have been added as promoters to Ni catalyst. Basically, different promoters accelerate reactions in different ways. Transition metals group commonly facilitate CO_2 conversion by assisting H_2 adsorption and dissociation, whereas alkaline earth metal improves Ni dispersion and prevents crystalline growth of NiO particles. La-promoted Ni catalyst was reported to introduce medium-strength basic sites for CO_2 adsorption [21]. On the other hand, Ce was commonly used because it can increase the oxygen vacancies to provide lattice defects that can improve oxygen mobilities and inhibit carbon deposition [97]. Figure 5 shows the literature survey on the types of second metals used and their performance in terms of CO_2 conversion.

Magnesium is among the typically used second metal to form bimetallic catalysts with Ni due to its strong basicity and high stability. MgO was utilized as a promoter for nanoparticles supported on silica in several studies [16,38,50] and found success as enhanced CH_4 selectivity and CO_2 conversion at optimum temperatures, and H_2/CO_2 ratio was observed in the presence of MgO. Theoretically, the presence of MgO can provide an alternative pathway by reacting with CO_2 to form magnesium carbonate, $MgCO_3$. $MgCO_3$ is the initial precursor to produce methane in which the H_2 is activated by active metal, as detailed by Park et al. [38]. This can also potentially minimize the CO byproduct by inhibiting CO desorption from the RWGS reaction. From the structural modification aspect, Guo and Lu [50] reported MgO influenced the Ni-based catalyst structure by forming NiO–MgO mixed-phase, thus the distribution of active sites is improved for CO_2 methanation. This is in agreement with the study by Meshkani and Rezaei [107], which indicated that the improved activity is possibly caused by the NiO–MgO solid solution formation and increment of basic sites. It is agreed that the introduction of Mg into Ni-based catalyst advances the reaction through sequential conversion of $CO_2{\rightarrow}CO{\rightarrow}CH_4$, following Equations (2) and (5) as in Table 1.

The Ni–Fe catalyst system, either as alloys or ferrites, is also active for CO_2 methanation purposes. Hwang et al. [44] studied the influence of various second metals (Fe, Zr, Mg, Y) on Ni/Al_2O_3 catalysts. Fe showed the best catalytic performance in terms of CO_2 conversion and CH_4 yield. This is postulated to be due to the $Ni–Fe/Al_2O_3$ catalyst retaining the weakest metal-support interaction. However, this is debatable, as no stability study was carried out because the lower interaction of metal with support is supposed to result in catalyst deactivation and Ni sintering. In another study by Ren et al. [18], $Ni–M/ZrO_2$ (M = Fe, Co, Cu) catalysts were comparatively studied, and the result also depicted Fe at 3% addition as the most efficient second metal. The enhanced performance of the reaction was hypothesized to be due to the strong-electron property of Fe, which promotes the reduction of Ni and ZrO_2 support. In most of the comparative studies on the effect of second metals, Fe can be concluded as the leading metal [108] but mechanistic studies on how Fe aid methanation is still limited.

As discussed earlier, Ru is the most active component for CO_2 methanation but the translation of research into the industrial application was limited due to its high price. Therefore, a study by Hwang et al. [109] has attempted to use Ru in a small amount as a promoter in a Ni-based catalyst system. Catalyst surface area was found to increase significantly with the addition of Ru up to 0.6% which is proportional to the amount of CO_2 converted. This, in turn, increases the CH_4 yield. The exploration of Ru as the second metal for the bimetallic catalyst system has not been widely investigated even though it is projected to be able to enhance the overall performance of the catalyst.

6. Reactor

Previous studies reported the use of different chemical reactors under specified operating conditions in which CO_2 methanation took place. Though, in most cases, the products that leave the methanation reactor contain both the desired methane and other undesired products. Hence, the reactor configuration and its operating conditions can be manipulated to improve the conversion of CO_2 and selectivity of CH_4. Under the presence of Ni-based catalyst, CO_2 and H_2 are fed into the reactor in which a heterogeneous reaction took place. Over the last 50 years, several methanations concepts have been developed using heterogeneous reactors.

Fixed-bed reactors are the most widely used two-phase reactor types in research, as well as industrial-commercial practice. The illustration of this reactor is shown in Figure 6. The fixed bed methanation reactor is composed of a cylindrical tube filled with either catalyst pellet or powder and is bathed by the reactant fluid (CO_2 and H_2) that flows uniformly through the bed and is being converted into products. Depending on the operation, apart from the single-bed reactor, several studies and industrial practices also reported using multiple-bed reactors. As methanation is a highly exothermic reaction that was first described by Sabatier in 1902 [110], the temperature control is achieved by using a series of adiabatic reactors, typically 2 to 5 bar, with inter-cooling and gas circulation [111]. Due to the adiabatic condition, temperature control became one of the limitations for this reactor. Rönsch et al. [23] also mentioned that fixed-bed reactors typically suffer quick temperature deviation, as the cooling system cannot adapt to a rapid change in the heat of the reaction. Hence, the main drawback of fixed-bed reactors is related to poor heat management, which resulted in the formation of temperature hot spots. This can obviously have detrimental outcomes on the operation of the reactor, such as catalyst deactivation, undesired side reactions, and thermal decomposition of the product [112]. Nevertheless, fixed-bed reactors also possess advantages, as it is vastly present for large-scale methanation applications. Moreover, a fixed-bed reactor shows better recyclability of catalyst as the solid catalyst in the reactor can be easily recovered. As a result, the catalytic activity of the catalyst can be restored to or near to its original performance, lowering the cost and time required to produce a new catalyst.
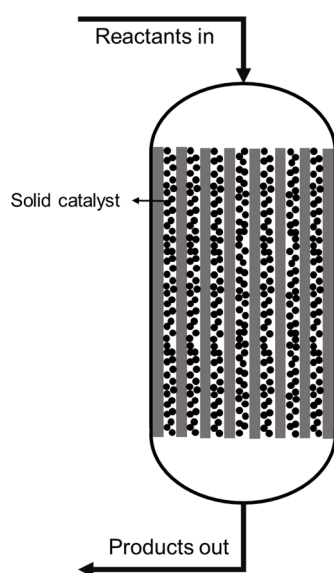
Figure 6. Illustration of the two-phase fixed-bed reactor.

Due to the high exothermic nature of methanation reaction, heat management is the major concern when designing a methanation reactor. Thus, this issue can be overcome by performing the reaction in a three-phase reactor, such as a slurry bubble column reactor (SBCR) and stirred-tank slurry reactor (CSTR). In SBCR, as shown in Figure 7, the gas

enters the reactor at the bottom and is distributed into the suspension of liquid products and catalyst by a distributor plate [113]. SBCRs operate mainly under isothermal conditions, with the heat of reaction removed through designed cooling tubes inserted in the reactor [113] or pipes with large surface areas for heat transfer to occur [114]. As previously mentioned, excellent reactor heat management can be achieved by using SBCR, making it ideal for CO_2 methanation and other exothermic reaction, such as Fischer–Tropsch synthesis, methanol, and dimethyl ether production [115]. Furthermore, previous work by de Swart et al. [113] has shown that SBCR has excellent heat management, with no severe temperature peaks or thermal runaway. SBCRs are often preferred over fixed-bed reactors and other reactors [114,116] due to their numerous advantages. These include flexible temperature control, excellent heat transfer, and efficient inter-phase contacting which results in higher productivity, low pressure drops leading to reduced compression costs, and better use of a catalyst (fine particles less than 100 μm) allowing better liquid-solid mass transfer [116]. However, SCBRs also have certain drawbacks, such as additional gas/liquid mass transfer resistance due to the liquid phase, which limits the effective reaction rate [117]. Therefore, the selection of types of liquid phases used is critical to improving gas solubility; hence enhancing the conversion. In a study by Lefbvre et al. [115], three different types of liquids namely squalene, octadecane, and dibenzyl toluene were used to study the influence of the liquid phase on the reaction kinetics. The study reveals the solubility of reactants differing in a different liquid with the highest gas solubility observed in dibenzyl toluene.
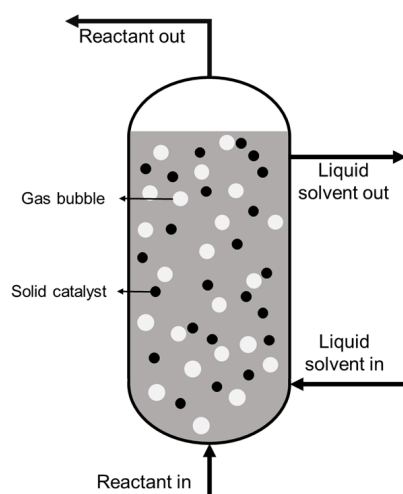
Figure 7. Illustration of three-phase slurry bubble column reactor.

A study on the comparison of two-phase and three-phase CO_2 methanation reaction kinetics was conducted by Lefebvre and Kolb [31]. The type of reactors that were used in the studies was a continuous stirred-tank slurry reactor (CSTR) and a fixed-bed reactor (FBR) under the presence of a commercial Ni/SiO_2 catalyst. The operating condition of both reactors was held constant to study if the presence of the liquid phase would affect the reaction kinetics. Based on the findings, the liquid phase employed in the three-phase methanation has a minimal relevant influence on the CO_2 methanation kinetic. Moreover, at the same temperature condition, the three-phase and two-phase reactors show comparable activation energy. This suggests that the performance of the three-phase reactor can yield similar results to that of a two-phase reactor, yet with better heat management. However, as of now, a limited number of industries and research employ the three-phase reactor for methanation due to limitations in the reusability of catalysts. Additionally, although the concept of SCBRs is relatively simple, the reactor design is highly complex and involves extensive knowledge of the reactor, which will lead to a difficulty in the scale-up later [116,117].

Generally, the reaction temperature, pressure, and gas feed ratio in the reactor would affect the CO_2 conversion and CH_4 selectivity. The two-phase reactor commonly operates at a relatively higher temperature of 300–500 °C compared to a two-phase reactor that operates under a lower temperature of 200–300 °C. A lower temperature is preferred for the liquid phase to improve the solubility of CO_2. The influence of temperature on the three-phase CSTR can be seen through the dependencies of Henry's law constant, $H_{i,pc}$, for H_2 and CO_2 in different types of liquids, as reported by Lefebvre et al. [115]. It can be observed that, for all liquids, H_2 solubility increases, while CO_2 solubility decreases with increasing temperature [115]. Meanwhile, pressure has a more significant effect on CO_2 methanation, the influence of temperature is more pronounced on the two-phase FBR CO_2 reaction rate. Overall, the optimization of the operation condition, such as temperature, pressure, gas feed, and the types of liquid must be tailored according to the type of reactor and catalyst used.

7. Mechanism of CO_2 Methanation

The catalytic pathway for CH_4 formation was still inconclusive, even though the mechanism has been intensively investigated. The major discrepancy is whether or not the Sabatier reaction forms CO as an intermediate [35] through the reaction sequence of Equations (2) and (3). From the previous research, mechanistic studies of CO_2 methanation are dichotomized into two methods, either through experimental approaches, such as in situ characterization using IR spectroscopy and DRIFTS, or the computational approach such as using DFT analysis. According to Aldana et al. [118], by using a Ni-based catalyst supported by Ce–Zr, H_2 was dissociated by Ni, whereas CO_2 was activated on the basic sites of support. The pathway for CH_4 formation is through the formate route ($CO_2 \rightarrow HCOO^- \rightarrow CH_3O^- \rightarrow CH_4$) without CO intermediate. This mechanism is supported by Pan et al. [119] However, there are disagreements on the mechanism in which Akamaru et al. [120], Park et al. [38], Eckle et al. and Karelovic et al. [121], suggested that CO_2 methanation proceeds via the formation of CO intermediates. On the other hand, Zhang et al. conducted in situ DRIFTS studies of CO_2 methanation, which indicates the CO_2 can be adsorbed to both support and Ni. The route in which the reaction took place depends on the %Ni loading on the support in which a lower concentration of nickel resulted in a high reverse-water gas shift (RWGS) reaction, indicating the reaction proceeds with CO intermediates. Conversely, the catalyst with a higher concentration of Ni shows favorable conversion to HCOO* as the intermediate species en route to methane yield [25]. Current progress found that active metal is responsible for H_2 dissociation, whereas CO_2 adsorption occurs either in the support or second metal. Many recent studies have explored in-depth chemical kinetics study and the use of computational chemistry and in situ characterization to understand the mechanism of CO_2 methanation. This is an important aspect because it is known that CO_2 activation energy, as well as the mechanism, is different when a different catalyst system is used. The combination of theoretical calculations and physical experiments would bridge the gap in the understanding of the reaction mechanism, which is of importance for tailoring the optimum conditions in a more efficient manner.

8. Conclusions

In this article, a comprehensive review of the progress and performance of Ni-based catalyst for CO_2 methanation has been outlined. As nickel nanoparticle is the best catalyst for CO_2 methanation, considering their high performance over cost ratio, further modification of Ni can enhance its performance. The modification of Ni catalysts, such as support, second metal, and synthesis parameters are thoroughly discussed. Upon this modification, physicochemical properties of the catalyst are affected; hence influencing their interaction with reactant and the composition of the final product. Due to the depletion of fossil fuels for energy use, the P2G technology is in demand.

Hydrogen production from water electrolysis is a mature technology that is widely implemented. Electrolysis technology includes alkaline electrolysis, proton exchange mem-

brane electrolysis (PEME), and solid oxide electrolysis cell (SOEC). The PEME technology has been widely commercialized by ITM Power in the United Kingdom in which the electrolyser is sold to different companies for a number of applications, including the P2G process [122]. CO_2 methanation, a component reaction in P2G technology, is a promising technology to decrease the high level of CO_2 in the atmosphere.

CO_2 methanation research has ramped up over the last century, as it is one of the most significant research projects with commercial and environmental benefits. For the implementation of CO_2 methanation, two points must be considered: (1) The reactor and catalyst for methanation must be able to operate at lower temperatures and give high methane yield as high temperatures cause a thermodynamic limitation; (2) the reaction mechanism of CO_2 methanation must be continuously studied to understand the route and intermediate formed so byproducts can be suppressed. CO_2 methanation is a well-known reaction that is being investigated as a carbon capture and storage (CCS) process and a renewable energy storage system based on a Power-to-Gas (P2G) conversion process using a substitute or synthetic natural gas (SNG). CO_2 methanation is critical to the effectiveness and efficiency of Power-to-Gas plants. The future of CO_2 methanation is vibrant, as the increased use of renewable energy sources necessitates the development of adequate storage systems to address the mismatch between power generation and instantaneous demand. In Germany, under the Audi in collaboration with ETOGAS GmbH, an industrial-scale P2G plant was developed in 2013, called the Audi e-gas project, in which CH_4 is synthesized and is being used to fuel up vehicles [123]. Furthermore, the efficiency of the Power-to-Gas system has been tested by thermally integrating high-temperature electrolysis (SOEC Technology) with methanation, with a predicted efficiency of more than 85%. This is conducted under the HELMETH project [124]. However, among the major challenges to widening the implementation of P2G, is the transportation and storage of the H_2 and CH_4 gases.

Author Contributions: M.S.S. and N.D.M.R. conducted the literature survey; N.D.M.R. and M.A.A. wrote the original draft preparation; M.S.S. supervised and administrated the work; M.S.S. and I.U.-D. revised, reviewed and edited the paper. All authors have read and agreed to the published version of the manuscript.

Conflicts of Interest: The authors declare no conflict of interest. The funders had no role in the design of the study; in the collection, analyses, or interpretation of data; in the writing of the manuscript, or in the decision to publish the results.

References

1. Gür, T.M. Carbon Dioxide Emissions, Capture, Storage and Utilization: Review of Materials, Processes and Technologies. *Prog. Energy Combust. Sci.* **2022**, *89*, 100965. [CrossRef]
2. Aziz, M.A.A.; Jalil, A.A.; Triwahyono, S.; Ahmad, A. CO_2 methanation over heterogeneous catalysts: Recent progress and future prospects. *Green Chem.* **2015**, *17*, 2647–2663. [CrossRef]
3. Al-Rowaili, F.N.; Zahid, U.; Onaizi, S.; Khaled, M.; Jamal, A.; Al-Mutairi, E.M. A review for Metal-Organic Frameworks (MOFs) utilization in capture and conversion of carbon dioxide into valuable products. *J. CO_2 Util.* **2021**, *53*, 101715. [CrossRef]
4. Cai, M.; Wen, J.; Chu, W.; Cheng, X.; Li, Z. Methanation of carbon dioxide on $Ni/ZrO_2-Al_2O_3$ catalysts: Effects of ZrO_2 promoter and preparation method of novel $ZrO_2-Al_2O_3$ carrier. *J. Nat. Gas Chem.* **2011**, *20*, 318–324. [CrossRef]
5. Gulzar, A.; Gulzar, A.; Ansari, M.B.; He, F.; Gai, S.; Yang, P. Carbon dioxide utilization: A paradigm shift with CO_2 economy. *Chem. Eng. J. Adv.* **2020**, *3*, 100013. [CrossRef]
6. Sodeifian, G.; Ardestani, N.S.; Sajadian, S.; Ghorbandoost, S. Application of supercritical carbon dioxide to extract essential oil from Cleome coluteoides Boiss: Experimental, response surface and grey wolf optimization methodology. *J. Supercrit. Fluids* **2016**, *114*, 55–63. [CrossRef]
7. Sodeifian, G.; Sajadian, S.A.; Derakhsheshpour, R. CO_2 utilization as a supercritical solvent and supercritical antisolvent in production of sertraline hydrochloride nanoparticles. *J. CO_2 Util.* **2022**, *55*, 101799. [CrossRef]
8. Sodeifian, G.; Razmimanesh, F.; Sajadian, S. Solubility measurement of a chemotherapeutic agent (Imatinib mesylate) in supercritical carbon dioxide: Assessment of new empirical model. *J. Supercrit. Fluids* **2019**, *146*, 89–99. [CrossRef]

9.   Ocampo, F.; Louis, B.; Kiwi-Minsker, L.; Roger, A.-C. Effect of Ce/Zr composition and noble metal promotion on nickel based CexZr1−xO2 catalysts for carbon dioxide methanation. *Appl. Catal. A Gen.* **2011**, *392*, 36–44. [CrossRef]

10. Park, J.H.; Yang, J.; Kim, D.; Gim, H.; Choi, W.Y.; Lee, J.W. Review of recent technologies for transforming carbon dioxide to carbon materials. *Chem. Eng. J.* **2022**, *427*, 130980. [CrossRef]

11. Götz, M.; Lefebvre, J.; Mörs, F.; McDaniel Koch, A.; Graf, F.; Bajohr, S.; Reimert, R.; Kolb, T. Renewable Power-to-Gas: A technological and economic review. *Renew. Energy* **2016**, *85*, 1371–1390. [CrossRef]

12. Frontera, P.; Macario, A.; Ferraro, M.; Antonucci, P. Supported Catalysts for CO_2 Methanation: A Review. *Catalysts* **2017**, *7*, 59. [CrossRef]

13. Su, X.; Xu, J.; Liang, B.; Duan, H.; Hou, B.; Huang, Y. Catalytic carbon dioxide hydrogenation to methane: A review of recent studies. *J. Energy Chem.* **2016**, *25*, 553–565. [CrossRef]

14. Ghaib, K.; Ben-Fares, F.-Z. Power-to-Methane: A state-of-the-art review. *Renew. Sustain. Energy Rev.* **2018**, *81*, 433–446. [CrossRef]

15. Fan, W.K.; Tahir, M. Recent trends in developments of active metals and heterogenous materials for catalytic CO_2 hydrogenation to renewable methane: A review. *J. Environ. Chem. Eng.* **2021**, *9*, 105460. [CrossRef]

16. Li, Y.; Lu, G.; Ma, J. Highly active and stable nano NiO–MgO catalyst encapsulated by silica with a core–shell structure for CO_2 methanation. *RSC Adv.* **2014**, *4*, 17420–17428. [CrossRef]

17. Aziz, M.; Jalil, A.; Triwahyono, S.; Mukti, R.; Taufiq-Yap, Y.; Sazegar, M. Highly active Ni-promoted mesostructured silica nanoparticles for CO_2 methanation. *Appl. Catal. B Environ.* **2014**, *147*, 359–368. [CrossRef]

18. Ren, J.; Qin, X.; Yang, J.-Z.; Qin, Z.-F.; Guo, H.-L.; Lin, J.-Y.; Li, Z. Methanation of carbon dioxide over Ni–M/ZrO2 (M = Fe, Co, Cu) catalysts: Effect of addition of a second metal. *Fuel Process. Technol.* **2015**, *137*, 204–211. [CrossRef]

19. Hu, F.; Ye, R.; Lu, Z.-H.; Zhang, R.; Feng, G. Structure–Activity Relationship of Ni-Based Catalysts toward CO_2 Methanation: Recent Advances and Future Perspectives. *Energy Fuels* **2021**, *36*, 156–169. [CrossRef]

20. Li, L.; Zeng, W.; Song, M.; Wu, X.; Li, G.; Hu, C. Research Progress and Reaction Mechanism of CO_2 Methanation over Ni-Based Catalysts at Low Temperature: A Review. *Catalysts* **2022**, *12*, 244. [CrossRef]

21. Stangeland, K.; Kalai, D.; Li, H.; Yu, Z. CO_2 Methanation: The Effect of Catalysts and Reaction Conditions. *Energy Procedia* **2017**, *105*, 2022–2027. [CrossRef]

22. Gao, J.; Wang, Y.; Ping, Y.; Hu, D.; Xu, G.; Gu, F.; Su, F. A thermodynamic analysis of methanation reactions of carbon oxides for the production of synthetic natural gas. *RSC Adv.* **2012**, *2*, 2358–2368. [CrossRef]

23. Rönsch, S.; Schneider, J.; Matthischke, S.; Schlüter, M.; Götz, M.; Lefebvre, J.; Prabhakaran, P.; Bajohr, S. Review on methanation— From fundamentals to current projects. *Fuel* **2016**, *166*, 276–296. [CrossRef]

24. Zhang, Z.; Tian, Y.; Zhang, L.; Hu, S.; Xiang, J.; Wang, Y.; Xu, L.; Liu, Q.; Zhang, S.; Hu, X. Impacts of nickel loading on properties, catalytic behaviors of Ni/γ–Al2O3 catalysts and the reaction intermediates formed in methanation of CO_2. *Int. J. Hydrogen Energy* **2019**, *44*, 9291–9306. [CrossRef]

25. Xu, L.; Wang, F.; Chen, M.; Nie, D.; Lian, X.; Lu, Z.; Chen, H.; Zhang, K.; Ge, P. CO_2 methanation over rare earth doped Ni based mesoporous catalysts with intensified low-temperature activity. *Int. J. Hydrogen Energy* **2017**, *42*, 15523–15539. [CrossRef]

26. Jia, X.; Zhang, X.; Rui, N.; Hu, X.; Liu, C.-J. Structural effect of Ni/ZrO2 catalyst on CO_2 methanation with enhanced activity. *Appl. Catal. B Environ.* **2019**, *244*, 159–169. [CrossRef]

27. Lin, J.; Ma, C.; Luo, J.; Kong, X.; Xu, Y.; Ma, G.; Wang, J.; Zhang, C.; Li, Z.; Ding, M. Preparation of Ni based mesoporous Al2O3 catalyst with enhanced CO_2 methanation performance. *RSC Adv.* **2019**, *9*, 8684–8694. [CrossRef]

28. Ahmad, W.; Younis, M.N.; Shawabkeh, R.; Ahmed, S. Synthesis of lanthanide series (La, Ce, Pr, Eu & Gd) promoted Ni/γ-Al2O3 catalysts for methanation of CO_2 at low temperature under atmospheric pressure. *Catal. Commun.* **2017**, *100*, 121–126. [CrossRef]

29. Guo, X.; He, H.; Traitangwong, A.; Gong, M.; Meeyoo, V.; Li, P.; Li, C.; Peng, Z.; Zhang, S. Ceria imparts superior low temperature activity to nickel catalysts for CO_2 methanation. *Catal. Sci. Technol.* **2019**, *9*, 5636–5650. [CrossRef]

30. Hamid, M.Y.S.; Jalil, A.A.; Rahman, A.F.A.; Abdullah, T.A.T. Enhanced reactive CO_2 species formation via V2O5-promoted Ni/KCC-1 for low temperature activation of CO_2 methanation. *React. Chem. Eng.* **2019**, *4*, 1126–1135. [CrossRef]

31. Lefebvre, J.; Bajohr, S.; Kolb, T. A comparison of two-phase and three-phase CO_2 methanation reaction kinetics. *Fuel* **2019**, *239*, 896–904. [CrossRef]

32. Jürgensen, L.; Ehimen, E.A.; Born, J.; Holm-Nielsen, J.B. Dynamic biogas upgrading based on the Sabatier process: Thermody- namic and dynamic process simulation. *Bioresour. Technol.* **2015**, *178*, 323–329. [CrossRef] [PubMed]

33. Zemansky, M.W.; Dittman, R.H. *Heat and Thermodynamics*; American Association of Physics Teachers: College Park, MD, USA, 1998.

34. Esa, Y.A.M.; Sapawe, N. A short review on carbon dioxide (CO_2) methanation process. *Mater. Today Proc.* **2020**, *31*, 394–397. [CrossRef]

35. Gao, J.; Liu, Q.; Gu, F.; Liu, B.; Zhong, Z.; Su, F. Recent advances in methanation catalysts for the production of synthetic natural gas. *RSC Adv.* **2015**, *5*, 22759–22776. [CrossRef]

36. Zhang, J.; Bai, Y.; Zhang, Q.; Wang, X.; Zhang, T.; Tan, Y.; Han, Y. Low-temperature methanation of syngas in slurry phase over Zr-doped Ni/γ-Al2O3 catalysts prepared using different methods. *Fuel* **2014**, *132*, 211–218. [CrossRef]

37. Hu, D.; Gao, J.; Ping, Y.; Jia, L.; Gunawan, P.; Zhong, Z.; Xu, G.; Gu, F.; Su, F. Enhanced Investigation of CO Methanation over Ni/Al2O3 Catalysts for Synthetic Natural Gas Production. *Ind. Eng. Chem. Res.* **2012**, *51*, 4875–4886. [CrossRef]

38. Park, J.-N.; Mc Farland, E.W. A highly dispersed Pd–Mg/SiO$_2$ catalyst active for methanation of CO$_2$. *J. Catal.* **2009**, *266*, 92–97. [CrossRef]

39. Tada, S.; Ochieng, O.J.; Kikuchi, R.; Haneda, T.; Kameyama, H. Promotion of CO$_2$ methanation activity and CH4 selectivity at low temperatures over Ru/CeO$_2$/Al$_2$O$_3$ catalysts. *Int. J. Hydrog Energy* **2014**, *39*, 10090–10100. [CrossRef]

40. Bligaard, T.; Nørskov, J.K.; Dahl, S.; Matthiesen, J.; Christensen, C.H.; Sehested, J. The Brønsted–Evans–Polanyi relation and the volcano curve in heterogeneous catalysis. *J. Catal.* **2004**, *224*, 206–217. [CrossRef]

41. Garbarino, G.; Bellotti, D.; Riani, P.; Magistri, L.; Busca, G. Methanation of carbon dioxide on Ru/Al$_2$O$_3$ and Ni/Al$_2$O$_3$ catalysts at atmospheric pressure: Catalysts activation, behaviour and stability. *Int. J. Hydrogen Energy* **2015**, *40*, 9171–9182. [CrossRef]

42. Zamani, A.; Ali, R.; Bakar, W.A. The investigation of Ru/Mn/Cu–Al$_2$O$_3$ oxide catalysts for CO$_2$/H$_2$ methanation in natural gas. *J. Taiwan Inst. Chem. Eng.* **2014**, *45*, 143–152. [CrossRef]

43. Kuznecova, I.; Gusca, J. Property based ranking of CO and CO$_2$ methanation catalysts. *Energy Procedia* **2017**, *128*, 255–260. [CrossRef]

44. Hwang, S.; Hong, U.G.; Lee, J.; Baik, J.H.; Koh, D.J.; Lim, H.; Song, I.K. Methanation of carbon dioxide over mesoporous nickel–M–alumina (M= Fe, Zr, Ni, Y, and Mg) xerogel catalysts: Effect of second metal. *Catal. Lett.* **2012**, *142*, 860–868. [CrossRef]

45. Muroyama, H.; Tsuda, Y.; Asakoshi, T.; Masitah, H.; Okanishi, T.; Matsui, T.; Eguchi, K. Carbon dioxide methanation over Ni catalysts supported on various metal oxides. *J. Catal.* **2016**, *343*, 178–184. [CrossRef]

46. Guo, X.; Traitangwong, A.; Hu, M.; Zuo, C.; Meeyoo, V.; Peng, Z.; Li, C. Carbon Dioxide Methanation over Nickel-Based Catalysts Supported on Various Mesoporous Material. *Energy Fuels* **2018**, *32*, 3681–3689. [CrossRef]

47. Ma, H.; Ma, K.; Ji, J.; Tang, S.; Liu, C.; Jiang, W.; Yue, H.; Liang, B. Graphene intercalated Ni-SiO2/GO-Ni-foam Catalyst with enhanced reactivity and heat-transfer for CO$_2$ methanation. *Chem. Eng. Sci.* **2019**, *194*, 10–21. [CrossRef]

48. Unwiset, P.; Chanapattharapol, K.C.; Kidkhunthod, P.; Poo-Arporn, Y.; Ohtani, B. Catalytic activities of titania-supported nickel for carbon-dioxide methanation. *Chem. Eng. Sci.* **2020**, *228*, 115955. [CrossRef]

49. Guo, M.; Lu, G. The difference of roles of alkaline-earth metal oxides on silica-supported nickel catalysts for CO$_2$ methanation. *RSC Adv.* **2014**, *4*, 58171–58177. [CrossRef]

50. Guo, M.; Lu, G. The effect of impregnation strategy on structural characters and CO$_2$ methanation properties over MgO modified Ni/SiO$_2$ catalysts. *Catal. Commun.* **2014**, *54*, 55–60. [CrossRef]

51. Carenco, S.; Tuxen, A.; Chintapalli, M.; Pach, E.; Escudero, C.; Ewers, T.D.; Jiang, P.; Borondics, F.; Thornton, G.; Alivisatos, A.P.; et al. Dealloying of Cobalt from CuCo Nanoparticles under Syngas Exposure. *J. Phys. Chem. C* **2013**, *117*, 6259–6266. [CrossRef]

52. Zhang, Y.; Chen, Y.; Liu, Q. Green synthesis of MCM-41 derived from renewable biomass and construction of VOx-Modified nickel phyllosilicate catalyst for CO$_2$ methanation. *Int. J. Hydrogen Energy* **2021**, *46*, 32003–32016. [CrossRef]

53. Hwang, S.; Hong, U.G.; Lee, J.; Gil Seo, J.; Baik, J.H.; Koh, D.J.; Lim, H.; Song, I.K. Methanation of carbon dioxide over mesoporous Ni–Fe–Al2O3 catalysts prepared by a coprecipitation method: Effect of precipitation agent. *J. Ind. Eng. Chem.* **2013**, *19*, 2016–2021. [CrossRef]

54. Zhan, Y.; Wang, Y.; Gu, D.; Chen, C.; Jiang, L.; Takehira, K. Ni/Al$_2$O$_3$-ZrO$_2$ catalyst for CO$_2$ methanation: The role of γ-(Al, Zr)2O$_3$ formation. *Appl. Surf. Sci.* **2018**, *459*, 74–79. [CrossRef]

55. Moghaddam, S.V.; Rezaei, M.; Meshkani, F.; Daroughegi, R. Synthesis of nanocrystalline mesoporous Ni/Al$_2$O$_3$SiO$_2$ catalysts for CO$_2$ methanation reaction. *Int. J. Hydrogen Energy* **2018**, *43*, 19038–19046. [CrossRef]

56. Quindimil, A.; De-La-Torre, U.; Pereda-Ayo, B.; Marcos, J.A.G.; González-Velasco, J.R. Ni catalysts with La as promoter supported over Y- and BETA- zeolites for CO$_2$ methanation. *Appl. Catal. B Environ.* **2018**, *238*, 393–403. [CrossRef]

57. Gac, W.; Zawadzki, W.; Słowik, G.; Sienkiewicz, A.; Kierys, A. Nickel catalysts supported on silica microspheres for CO$_2$ methanation. *Microporous Mesoporous Mater.* **2018**, *272*, 79–91. [CrossRef]

58. Ratchahat, S.; Sudoh, M.; Suzuki, Y.; Kawasaki, W.; Watanabe, R.; Fukuhara, C. Development of a powerful CO$_2$ methanation process using a structured Ni/CeO$_2$ catalyst. *J. CO$_2$ Util.* **2018**, *24*, 210–219. [CrossRef]

59. Hu, L.; Urakawa, A. Continuous CO$_2$ capture and reduction in one process: CO$_2$ methanation over unpromoted and promoted Ni/Zr, O$_2$. *J. CO$_2$ Util.* **2018**, *25*, 323–329. [CrossRef]

60. Wang, X.; Zhu, L.; Liu, Y.; Wang, S. CO$_2$ methanation on the catalyst of Ni/MCM-41 promoted with CeO$_2$. *Sci. Total Environ.* **2018**, *625*, 686–695. [CrossRef]

61. Le, T.A.; Kim, T.W.; Lee, S.H.; Park, E.D. Effects of Na content in Na/Ni/SiO$_2$ and Na/Ni/CeO$_2$ catalysts for CO and CO$_2$ methanation. *Catal. Today* **2018**, *303*, 159–167. [CrossRef]

62. Zhou, G.; Liu, H.; Cui, K.; Jia, A.; Hu, G.; Jiao, Z.; Liu, Y.; Zhang, X. Role of surface Ni and Ce species of Ni/CeO$_2$ catalyst in CO$_2$ methanation. *Appl. Surf. Sci.* **2016**, *383*, 248–252. [CrossRef]

63. Danaci, S.; Protasova, L.; Lefevere, J.; Bedel, L.; Guilet, R.; Marty, P. Efficient CO$_2$ methanation over Ni/Al 2 O 3 coated structured catalysts. *Catal. Today* **2016**, *273*, 234–243. [CrossRef]

64. Dias, Y.R.; Perez-Lopez, O.W. Carbon dioxide methanation over Ni-Cu/SiO$_2$ catalysts. *Energy Convers. Manag.* **2020**, *203*, 112214. [CrossRef]

65. Varvoutis, G.; Lykaki, M.; Stefa, S.; Binas, V.; Marnellos, G.E.; Konsolakis, M. Deciphering the role of Ni particle size and nickel-ceria interfacial perimeter in the low-temperature CO$_2$ methanation reaction over remarkably active Ni/CeO$_2$ nanorods. *Appl. Catal. B Environ.* **2021**, *297*, 120401. [CrossRef]

66. Ye, R.-P.; Li, Q.; Gong, W.; Wang, T.; Razink, J.J.; Lin, L.; Qin, Y.-Y.; Zhou, Z.; Adidharma, H.; Tang, J.; et al. High-performance of nanostructured Ni/CeO$_2$ catalyst on CO$_2$ methanation. *Appl. Catal. B Environ.* **2020**, *268*, 118474. [CrossRef]

67. Ridzuan, N.D.M.; Shaharun, M.S.; Lee, K.M.; Din, I.U.; Puspitasari, P. Influence of Nickel Loading on Reduced Graphene Oxide-Based Nickel Catalysts for the Hydrogenation of Carbon Dioxide to Methane. *Catalysts* **2020**, *10*, 471. [CrossRef]

68. Gac, W.; Zawadzki, W.; Rotko, M.; Greluk, M.; Słowik, G.; Kolb, G. Effects of support composition on the performance of nickel catalysts in CO$_2$ methanation reaction. *Catal. Today* **2020**, *357*, 468–482. [CrossRef]

69. Summa, P.; Samojeden, B.; Motak, M.; Wierzbicki, D.; Alxneit, I.; Świerczek, K.; Da Costa, P. Investigation of Cu promotion effect on hydrotalcite-based nickel catalyst for CO$_2$ methanation. *Catal. Today* **2022**, *384–386*, 133–145. [CrossRef]

70. Summa, P.; Świrk, K.; Wang, Y.; Samojeden, B.; Rønning, M.; Hu, C.; Motak, M.; Da Costa, P. Effect of cobalt promotion on hydrotalcite-derived nickel catalyst for CO$_2$ methanation. *Appl. Mater. Today* **2021**, *25*, 101211. [CrossRef]

71. Gac, W.; Zawadzki, W.; Słowik, G.; Kuśmierz, M.; Dzwigaj, S. The state of BEA zeolite supported nickel catalysts in CO$_2$ methanation reaction. *Appl. Surf. Sci.* **2021**, *564*, 150421. [CrossRef]

72. Gholami, S.; Alavi, S.M.; Rezaei, M. Synthesis of Cr$_2$O$_3$–Al$_2$O$_3$ powders with various Cr$_2$O$_3$/Al$_2$O$_3$ molar ratios and their applications as support for the preparation of nickel catalysts in CO$_2$ methanation reaction. *Int. J. Hydrogen Energy* **2021**, *46*, 5311–5322. [CrossRef]

73. Taherian, Z.; Khataee, A.; Orooji, Y. Promoted nickel-based catalysts on modified mesoporous silica support: The role of yttria and magnesia on CO$_2$ methanation. *Microporous Mesoporous Mater.* **2020**, *306*, 110455. [CrossRef]

74. Aljishi, A.; Veilleux, G.; Lalinde, J.A.H.; Kopyscinski, J. The effect of synthesis parameters on ordered mesoporous nickel alumina catalyst for CO$_2$ methanation. *Appl. Catal. A Gen.* **2018**, *549*, 263–272. [CrossRef]

75. Sun, J.; Wang, Y.; Zou, H.; Guo, X.; Wang, Z.-J. Ni catalysts supported on nanosheet and nanoplate γ-Al$_2$O$_3$ for carbon dioxide methanation. *J. Energy Chem.* **2019**, *29*, 3–7. [CrossRef]

76. Hu, F.; Tong, S.; Lu, K.; Chen, C.-M.; Su, F.-Y.; Zhou, J.; Lu, Z.-H.; Wang, X.; Feng, G.; Zhang, R. Reduced graphene oxide supported Ni-Ce catalysts for CO$_2$ methanation: The support and ceria promotion effects. *J. CO$_2$ Util.* **2019**, *34*, 676–687. [CrossRef]

77. Liao, L.; Chen, L.; Ye, R.; Tang, X.; Liu, J. Robust nickel silicate catalysts with high Ni loading for CO$_2$ methanation. *Chem. Asian J.* **2021**, *16*, 678–689. [CrossRef]

78. Liu, C.-J.; Ye, J.; Jiang, J.; Pan, Y. Progresses in the Preparation of Coke Resistant Ni-based Catalyst for Steam and CO$_2$ Reforming of Methane. *ChemCatChem* **2011**, *3*, 529–541. [CrossRef]

79. Wierzbicki, D.; Dębek, R.; Motak, M.; Grzybek, T.; Galvez, M.E.; Da Costa, P. Novel Ni-La-hydrotalcite derived catalysts for CO$_2$ methanation. *Catal. Commun.* **2016**, *83*, 5–8. [CrossRef]

80. Abate, S.; Barbera, K.; Giglio, E.; Deorsola, F.; Bensaid, S.; Perathoner, S.; Pirone, R.; Centi, G. Synthesis, Characterization, and Activity Pattern of Ni–Al Hydrotalcite Catalysts in CO$_2$ Methanation. *Ind. Eng. Chem. Res.* **2016**, *55*, 8299–8308. [CrossRef]

81. Wu, J.; Jin, Z.; Wang, B.; Han, Y.; Xu, Y.; Liang, Z.; Wang, Z. Nickel Nanoparticles Encapsulated in Microporous Graphenelike Carbon (Ni@MGC) as Catalysts for CO$_2$ Methanation. *Ind. Eng. Chem. Res.* **2019**, *58*, 20536–20542. [CrossRef]

82. Riani, P.; Garbarino, G.; Lucchini, M.A.; Canepa, F.; Busca, G. Unsupported versus alumina-supported Ni nanoparticles as catalysts for steam/ethanol conversion and CO$_2$ methanation. *J. Mol. Catal. A Chem.* **2014**, *383–384*, 10–16. [CrossRef]

83. Lin, J.; Ma, C.; Wang, Q.; Xu, Y.; Ma, G.; Wang, J.; Wang, H.; Dong, C.; Zhang, C.; Ding, M. Enhanced low-temperature performance of CO$_2$ methanation over mesoporous Ni/Al$_2$O$_3$-ZrO$_2$ catalysts. *Appl. Catal. B Environ.* **2019**, *243*, 262–272. [CrossRef]

84. Liu, Q.; Bian, B.; Fan, J.; Yang, J. Cobalt doped Ni based ordered mesoporous catalysts for CO$_2$ methanation with enhanced catalytic performance. *Int. J. Hydrogen Energy* **2018**, *43*, 4893–4901. [CrossRef]

85. Xu, L.; Lian, X.; Chen, M.; Cui, Y.; Wang, F.; Li, W.; Huang, B. CO$_2$ methanation over Co Ni bimetal-doped ordered mesoporous Al$_2$O$_3$ catalysts with enhanced low-temperature activities. *Int. J. Hydrogen Energy* **2018**, *43*, 17172–17184. [CrossRef]

86. Mihet, M.; Lazar, M.D. Methanation of CO$_2$ on Ni/γ-Al$_2$O$_3$: Influence of Pt, Pd or Rh promotion. *Catal. Today* **2018**, *306*, 294–299. [CrossRef]

87. Daroughegi, R.; Meshkani, F.; Rezaei, M. Enhanced activity of CO$_2$ methanation over mesoporous nanocrystalline Ni–Al2O3 catalysts prepared by ultrasound-assisted co-precipitation method. *Int. J. Hydrogen Energy* **2017**, *42*, 15115–15125. [CrossRef]

88. Ravenelle, R.M.; Copeland, J.R.; Kim, W.G.; Crittenden, J.C.; Sievers, C. Structural changes of γ-Al$_2$O$_3$-supported catalysts in hot liquid water. *Acs Catal.* **2011**, *1*, 552–561. [CrossRef]

89. Bai, X.; Wang, S.; Sun, T.; Wang, S. The sintering of Ni/Al$_2$O$_3$ methanation catalyst for substitute natural gas production. *React. Kinet. Mech. Catal.* **2014**, *112*, 437–451. [CrossRef]

90. Bacariza, M.C.; Graça, I.; Bebiano, S.S.; Lopes, J.M.; Henriques, C. Magnesium as Promoter of CO$_2$ Methanation on Ni-Based USY Zeolites. *Energy Fuels* **2017**, *31*, 9776–9789. [CrossRef]

91. Le, T.A.; Kim, M.S.; Lee, S.H.; Kim, T.W.; Park, E.D. CO and CO$_2$ methanation over supported Ni catalysts. *Catal. Today* **2017**, *293–294*, 89–96. [CrossRef]

92. Yamasaki, M.; Habazaki, H.; Yoshida, T.; Akiyama, E.; Kawashima, A.; Asami, K.; Hashimoto, K.; Komori, M.; Shimamura, K. Compositional dependence of the CO$_2$ methanation activity of Ni/ZrO$_2$ catalysts prepared from amorphous NiZr alloy precursors. *Appl. Catal. A Gen.* **1997**, *163*, 187–197. [CrossRef]

93. HPabazaki, H. Amorphous iron group metal- valve metal alloy catalysts for hydrogenation of carbon dioxide. *Electrochem. Soc. Inc. Corros. Electrochem. Catal. Metastable Met. Internet. (USA)* **1993**, *1993*, 393–404.

94. Ren, J.; Li, H.; Jin, Y.; Zhu, J.; Liu, S.; Lin, J.; Li, Z. Silica/titania composite-supported Ni catalysts for CO methanation: Effects of Ti species on the activity, anti-sintering, and anti-coking properties. *Appl. Catal. B Environ.* **2017**, *201*, 561–572. [CrossRef]
95. Jia, C.; Dai, Y.; Yang, Y.; Chew, J.W. Nickel cobalt catalyst supported on TiO_2-coated SiO_2 spheres for CO_2 methanation in a fluidized bed. *Int. J. Hydrogen Energy* **2019**, *44*, 13443–13455. [CrossRef]
96. Vrijburg, W.L.; Moioli, E.; Chen, W.; Zhang, M.; Terlingen, B.J.; Zijlstra, B.; Filot, I.A.; Züttel, A.; Pidko, E.A.; Hensen, E.J. Efficient Base-Metal $NiMn/TiO_2$ Catalyst for CO_2 Methanation. *ACS Catal.* **2019**, *9*, 7823–7839. [CrossRef]
97. Wang, W.; Chu, W.; Wang, N.; Yang, W.; Jiang, C. Mesoporous nickel catalyst supported on multi-walled carbon nanotubes for carbon dioxide methanation. *Int. J. Hydrogen Energy* **2016**, *41*, 967–975. [CrossRef]
98. Marcano, D.C.; Kosynkin, D.V.; Berlin, J.M.; Sinitskii, A.; Sun, Z.; Slesarev, A.; Alemany, L.B.; Lu, W.; Tour, J.M. Improved Synthesis of Graphene Oxide. *ACS Nano* **2010**, *4*, 4806–4814. [CrossRef]
99. Novoselov, K.S.; Geim, A.K.; Morozov, S.V.; Jiang, D.; Zhang, Y.; Dubonos, S.V.; Grigorieva, I.V.; Firsov, A.A. Electric field effect in atomically thin carbon films. *Science* **2004**, *306*, 666–669. [CrossRef]
100. Park, S.; An, J.; Potts, J.R.; Velamakanni, A.; Murali, S.; Ruoff, R.S. Hydrazine-reduction of graphite- and graphene oxide. *Carbon* **2011**, *49*, 3019–3023. [CrossRef]
101. Din, I.U.; Shaharun, M.; Subbarao, D.; Naeem, A. Synthesis, characterization and activity pattern of carbon nanofibers based copper/zirconia catalysts for carbon dioxide hydrogenation to methanol: Influence of calcination temperature. *J. Power Sources* **2015**, *274*, 619–628. [CrossRef]
102. Din, I.U.; Shaharun, M.; Subbarao, D.; Naeem, A.; Hussain, F. Influence of niobium on carbon nanofibres based Cu/ZrO 2 catalysts for liquid phase hydrogenation of CO_2 to methanol. *Catal. Today* **2016**, *259*, 303–311. [CrossRef]
103. Deerattrakul, V.; Dittanet, P.; Sawangphruk, M.; Kongkachuichay, P. CO_2 hydrogenation to methanol using Cu-Zn catalyst supported on reduced graphene oxide nanosheets. *J. CO_2 Util.* **2016**, *16*, 104–113. [CrossRef]
104. Jiménez, V.; Sánchez, P.; Panagiotopoulou, P.; Valverde, J.L.; Romero, A. Methanation of CO, CO_2 and selective methanation of CO, in mixtures of CO and CO_2, over ruthenium carbon nanofibers catalysts. *Appl. Catal. A Gen.* **2010**, *390*, 35–44. [CrossRef]
105. Julkapli, N.M.; Bagheri, S. Graphene supported heterogeneous catalysts: An overview. *Int. J. Hydrogen Energy* **2015**, *40*, 948–979. [CrossRef]
106. Yuan, H.; Zhu, X.; Han, J.; Wang, H.; Ge, Q. Rhenium-promoted selective CO_2 methanation on Ni-based catalyst. *J. CO_2 Util.* **2018**, *26*, 8–18. [CrossRef]
107. Meshkani, F.; Rezaei, M. Nanocrystalline MgO supported nickel-based bimetallic catalysts for carbon dioxide reforming of methane. *Int. J. Hydrogen Energy* **2010**, *35*, 10295–10301. [CrossRef]
108. Hwang, S.; Lee, J.; Hong, U.G.; Jung, J.C.; Koh, D.J.; Lim, H.; Byun, C.; Song, I.K. Hydrogenation of carbon monoxide to methane over mesoporous nickel-M-alumina (M=Fe, Ni, Co, Ce, and La) xerogel catalysts. *J. Ind. Eng. Chem.* **2012**, *18*, 243–248. [CrossRef]
109. Hwang, S.; Lee, J.; Hong, U.G.; Baik, J.H.; Koh, D.J.; Lim, H.; Song, I.K. Methanation of carbon dioxide over mesoporous $Ni–Fe–Ru–Al_2O_3$ xerogel catalysts: Effect of ruthenium content. *J. Ind. Eng. Chem.* **2013**, *19*, 698–703. [CrossRef]
110. Held, M.; Schollenberger, D.; Sauerschell, S.; Bajohr, S.; Kolb, T. Methanation Concepts for SNG Production at the Engler-Bunte-Institut. *Chem. Ing. Tech.* **2020**, *92*, 595–602. [CrossRef]
111. Lefebvre, J.; Götz, M.; Bajohr, S.; Reimert, R.; Kolb, T. Improvement of three-phase methanation reactor performance for steady-state and transient operation. *Fuel Process. Technol.* **2015**, *132*, 83–90. [CrossRef]
112. Bendjaouahdou, C.; Bendjaouahdou, M.H. Control of the Hot Spot Temperature in an Industrial SO_2 Converter. *Energy Procedia* **2013**, *36*, 428–443. [CrossRef]
113. De Swart, J.; Krishna, R. Simulation of the transient and steady state behaviour of a bubble column slurry reactor for Fischer–Tropsch synthesis. *Chem. Eng. Process. Process Intensif.* **2002**, *41*, 35–47. [CrossRef]
114. Basha, O.M.; Morsi, B.I. CFD for the Design and Optimization of Slurry Bubble Column Reactors. In *Computational Fluid Dynamics—Basic Instruments and Applications in Science*; InTech: London, UK, 2018.
115. Lefebvre, J.; Trudel, N.; Bajohr, S.; Kolb, T. A study on three-phase CO_2 methanation reaction kinetics in a continuous stirred-tank slurry reactor. *Fuel* **2018**, *217*, 151–159. [CrossRef]
116. Seyednejadian, S.; Rauch, R.; Bensaid, S.; Hofbauer, H.; Weber, G.; Saracco, G. Power to Fuels: Dynamic Modeling of a Slurry Bubble Column Reactor in Lab-Scale for Fischer Tropsch Synthesis under Variable Load of Synthesis Gas. *Appl. Sci.* **2018**, *8*, 514. [CrossRef]
117. Lefebvre, J. *Three-phase CO_2 Methanation: Methanation Reaction Kinetics and Transient Behavior of a Slurry Bubble Column Reactor, in Fakultät für Chemieingenieurwesen und Verfahrenstechnik*; Karlsruher Instituts für Technologie: Karlsruhe, Germany, 2019.
118. Ussa, P.A.; Ocampo, F.; Kobl, K.; Louis, B.; Thibault-Starzyka, F.; Daturi, M.; Bazin, P.; Thomas, S.; Roger, A.C. Catalytic CO_2 valorization into CH4 on Ni-based ceria-zirconia. Reaction mechanism by operando IR spectroscopy. *Catal. Today* **2013**, *215*, 201–207. [CrossRef]
119. Pan, Q.; Peng, J.; Sun, T.; Wang, S.; Wang, S. Insight into the reaction route of CO_2 methanation: Promotion effect of medium basic sites. *Catal. Commun.* **2014**, *45*, 74–78. [CrossRef]
120. Akamaru, S.; Shimazaki, T.; Kubo, M.; Abe, T. Density functional theory analysis of methanation reaction of CO_2 on Ru nanoparticle supported on TiO_2 (101). *Appl. Catal. A Gen.* **2014**, *470*, 405–411. [CrossRef]
121. Karelovic, A.; Ruiz, P. Mechanistic study of low temperature CO_2 methanation over Rh/TiO_2 catalysts. *J. Catal.* **2013**, *301*, 141–153. [CrossRef]

122. Protecting Finite Natural Gas Stores with Green Hydrogen. Green Hydrogen for Methanation. 2022. Available online: https://itm-power.com/markets/hydrogen-for-methanation (accessed on 19 April 2022).

123. Audi Opens Power-to-Gas Facility in Werlte/Emsland; e-Gas from Water, Green Electricity and CO_2. 2013. Available online: https://www.greencarcongress.com/2013/06/audi-20130625.html (accessed on 19 April 2022).

124. HELMETH Integrated High-Temperature ELectrolysis and METHanation for Effective Power to Gas Conversion. Project 2022. Available online: http://www.helmeth.eu/index.php/project (accessed on 19 April 2022).